The LVD signals during the early-mid stages of the L'Aquila seismic sequence and the radon signature of some aftershocks of moderate magnitude

(Article begins on next page)

27 September 2024

UNIVERSITÀ DEGLI STUDI DI TORINO

Cigolini C., Laiolo M., Coppola D. (2014) The LVD signals during the early-mid stages of the L'Aquila seismic sequence and the radon signature of some aftershocks of moderate magnitude. Journal of Environmental Radioactivity, 139,56-65. http://dx.doi.org/10.1016/j.jenvrad.2014.09.017

The LVD signals during the early-mid stages of the L'Aquila seismic sequence and the radon signature of some aftershocks of moderate magnitude

Cigolini C.[1,2], Laiolo M.[1,3], Coppola D.[1]

1 – Dipartimento di Scienze della Terra, Università di Torino,Via Valperga Caluso 35, 10125 Torino, Italy
2 –NatRisk, Centro Interdipartimentale sui Rischi Naturali in Ambiente Montano e Collinare, Università degli Studi di Torino, Italy
3 – Dipartimento di Scienze della Terra, Università di Firenze, Via Giorgio La Pira 4, 50121 Firenze, Italy

Correspondig Author: Corrado Cigolini
Email: corrado.cigolini@unito.it; Phone: +39-011670-5107; Fax: +39-011670-5128

Highlight

1) The April 9, 2009 Aquila earthquake (ML 5.9) had a remarkable echo in the media

2) We report LVD traces together with the data of a radon monitoring experiment

3) Radon emissions were measured by 3 automatic stations along the main NW-SE fault

4) The one that better responds to seismicity was placed in the fault's bedrock

5) Future networks for earthquake radon monitoring should implement this setting

1   **The LVD signals during the early-mid stages of the L'Aquila seismic sequence and the radon**

2   **signature of some aftershocks of moderate magnitude**

3

4   Cigolini C.[1,2], Laiolo M.[1,3], Coppola D.[1]

5   1 – Dipartimento di Scienze della Terra, Università di Torino,Via Valperga Caluso 35, 10125 Torino, Italy
6   2 –NatRisk, Centro Interdipartimentale sui Rischi Naturali in Ambiente Montano e Collinare, Università
7   degli Studi di Torino, Italy
8   3 – Dipartimento di Scienze della Terra, Università di Firenze, Via Giorgio La Pira 4, 50121 Firenze, Italy
9

10   Correspondig Author: Corrado Cigolini
11   Email: corrado.cigolini@unito.it; Phone: +39-011670-5107; Fax: +39-011670-5128
12

13   Key words: *LVD traces, radon monitoring, earthquake precursors, networks for radon monitoring*

14   **Abstract**

15   The L'Aquila seismic swarm culminated with the mainshock of April 6, 2009 (M_L=5.9). Here, we

16   report and analyze the Large Volume Detector (LVD, used in neutrinos research) low energy traces

17   (~0.8 MeV), collected during the early-mid stages of the seismic sequence, together with the data of

18   a radon monitoring experiment. The peaks of LVD traces do not correlate with the evolution and

19   magnitude of earthquakes, including major aftershocks. Conversely, our radon measurements

20   obtained by utilizing three automatic stations deployed along the regional NW-SE faulting system,

21   seem to be, in one case, more efficient. In fact, the timeseries collected on the NW-SE Paganica

22   fracture recorded marked variations and peaks that occurred during and prior moderate aftershocks

23   (with M_L>3). The Paganica monitoring station (PGN) better responds to active seismicity due to the

24   fact that the radon detector was placed directly within the bedrock of an active fault. It is suggested

25   that future networks for radon monitoring of active seismicity should preferentially implement this

26   setting.

27

28   **Introduction**

29   The L'Aquila seismic swarm affected the Abruzzo region in Central Italy since December 2008 to

30   September 2009 (Fig. 1). During the seismic sequence a major earthquake hit the city of Aquila on

31   April 6 of that year (at 01:32 UTC) causing 309 victims (Amato et al., 2011). The magnitude of the

32   event was rated ML 5.9 on the Richter scale with a moment magnitude Mw 6.3. In the light of this

33   parameter this was the ninth stronger earthquake since the beginning of the XXth century (Table 1).

34   Several thousand foreshocks and aftershocks were recorded by the Istituto Nazionale di Geofisica e

35   Vulcanologia (INGV), and more than 30 events had a magnitude higher than 3.5 (Chiaraluce et al.,

36   2011). Major aftershocks occurred on April 7 and April 9, with magnitudes (M_L) of 5.3 and 5.1,

37   respectively.

38

39   **Fig. 1 and Table 1**

40

41   The major earthquake was triggered by the motion of a NW-SE trending normal fault parallel to the

42   trending of the Apennines central axis (Akinci et al., 2009; Herrmann et al., 2011). The depth of the

43   hypocenter was estimated to be at about 9.5 km (Latitude 42.3476°N, Longitude13.3800 E;

44   Chiaraluce et al., 2011 among others). The central part of the Apennines has been characterized by

45   extensional tectonics since Pliocene times due to the faster opening of the back-arc basin

46   (Tyrrhenian sea) compared with the rates of plate convergence, the latter associated with the

47   collision of the Adria microplate with the major Eurasian plate. (e.g., Riguzzi et al., 2013).

48   The Aquila earthquake had a remarkable echo in the media due to the fact that G. Giuliani claimed

49   that he could have predicted, by means of radon data, the April 6, 2009 earthquake (cf. its

50   reconstruction of the events summarized in an informative monograph: Giuliani, 2009). Within the

51   same year, the International Commission on Earthquake Forecasting for Civil Protection, after

52   interviewing him, concluded, also in the light of the available geophysical data collected by other

53   groups of scientists, that there were "no convincing evidence of diagnostic precursors" of the

54   mainshock before its occurrence (Jordan et al., 2009, p. 323 and p. 361). An additional issue on the

55   Aquila earthquake is related to the fact that seven experts were each sentenced "for downplaying

56   seismic risk" before the occurrence of the deadly event (Cartlidge, 2014). Currently, an appeal on

57   this case is pending.

58   Beside radon, several other signals, some of them precursory, were reported after the main event,

59   such as earthquake lights (Fidani, 2010), variations in the intensity of radio waves in the LF and

60   VLF bands (Biagi et al., 2009; Rozhnoi et al., 2009), thermal anomalies onto seismogenetic areas

61   (Pergola et al., 2010; Genzano et al., 2009), small mud volcanoes in the Aterno valley (De Martini

62   et al., 2012), "storms of crustal stress" and acoustic emissions (Gregori et al., 2010), electric field

63   anomalies (Fidani, 2010), and uranium (U) groundwater anomalies (Plastino et al., 2010).

64   In addition, Bonfanti et al. (2012) discussed the relationships between seismicity and CO_2 - CH_4

65   degassing during the main seismic sequences that affected Central Appenines within the last two

66   decades. However, several authors emphasized the possible role of "large-scale pockets of high

67   fluid pressure" in the triggering of l'Aquila seismic sequence (Terakawa et al., 2010), as well as the

68   one of Colfiorito, during 1996-1997 (Di Luccio et al., 2010, Lucente et al., 2010). Moreover,

69   Chiodini et al. (2011) found an increase of radiogenic isotopes of crustal origin (^{4}He and ^{40}Ar) in

70   local water tables, likely related to the structural setting of the region.

71   However, Pulinets et al. (2009) suggested a correlation between the ionization of the near ground

72   layer of the atmosphere and radon emissions at l'Aquila (since its decay products may become

73   clusters for water condensation and local temperature anomalies as suggested by Ouzounov and

74   Freund, 2004).

75   Radon is radioactive gas generated from the decay of uranium bearing rocks, soils and magmas.

76   The role of radon as a potential precursor of earthquake has been extensively debated. It is generally

77   accepted that anomalous radon emissions, together with those of other geochemical and geophysical

78   parameters, may be released prior an earthquake (Toutain and Baubron, 1999; Kumar et al., 2009).

79   Peaks in radon concentrations before, during and after the onset of tectonic earthquakes (up to 1200

80   % background values) have been reported in literature since the early sixties (Cicerone et al., 2009).

81   Radon is also considered as an indicator of crustal stress regimes (e.g., Steinitz et al, 2003; Trique et

82   al., 1999). In summary, the radon-earthquake relationships can be correlated to stress regimes,

83   fracturing and microfracturing of crustal rocks (e.g., Hishimuma et al., 1999; Tuccimei et al., 2010)

84   in preparing the ground for the development of a seismic event, during its onset and/or after its

85   occurrence.

86   In nature, radon is essentially present as ^{222}Rn (with a half life of 3.82 days) and its anomalies were

87   observed before, during and after the onset of regional seismic events (e.g., Scholtz et al., 1973;

88   Fleischer and Mogro-Campero, 1985; Igarashi et al., 1995; Richon et al, 2003; Planinić et al., 2004;

89   Crockett et al., 2006; Kawada et al., 2007; Ghosh et al., 2009; Cigolini, 2010). Variations in radon

90   emissions were also observed during changes in volcanic activity and volcanically-related

91   earthquakes at Hawaii (Cox, 1980; Thomas et al., 1986). Cigolini et al. (2001) were able, by

92   utilizing a network of measuring stations at Mount Vesuvius, to discriminate ^{222}Rn anomalies due to

93   regional earthquakes from those related to volcanic seismicity. However, Burton et al. (2004)

94   performed systematic radon measurements at Mount Etna (during the seismic sequence of October,

95   2002) and decoded the trend and extension of a hidden fault. Relationships between seismogenic

96   faults and radon emissions have been recently investigated by several authors (Vaupotiĉ et al.,

97   2010; Papastefanou, 2010), whereas Reddy et al. (2004) found a correlation between the increase of

98   radon concentrations and microseismicity in a stable continental region. Moreover, Cigolini et al.

99   (2007) detected earthquake-volcano interactions at Stromboli volcano: in this case radon anomalies

100   were precursory, coseismic and somehow delayed in respect to the onset of regional seismic events.

101   However, the anomalies of radon signal are better suited to forecast eruptive episodes since we

102   know the loci of volcanic eruptions and we can follow the evolution of volcanic activity (e.g.,

103   Chirkov, 1975; Connors et al., 1996; Alparone et al., 2005; Cigolini et al., 2005; 2013). Conversely,

104   its role as a precursor of earthquakes is more controversial since we do not know when and where

105   the earthquake is going to hit.

106   Several works show that environmental parameters are critical in modulating radon emissions (e.g.,

107   Mogro-Campero and Fleischer, 1977; Pinault and Baubron, 1996; Planinić et al., 2001; Pérez et al.,

108   2007; Cigolini et al., 2009). Automatic and real-time measurements substantially increase the

109   potential role of radon in earthquake prediction since the data are may be easily collected,

110   transferred, elaborated and filtered thus minimizing the interference of environmental parameters

111 (Cigolini et al., 2009; Laiolo et al., 2012). Therefore, time series analysis of the ^{222}Rn signal allow

112 us to better track radon degassing in space and time.

113 In this paper we are revisiting some Large Volume Detectors (LVD) data collected at the

114 "Laboratori Nazionali del Gran Sasso, LNGS" (Gran Sasso National Laboratories) in the attempt to

115 infer radon variations during the evolution of the seismic sequence. LVD are large volume liquid

116 scintillator detectors created to search for neutrinos from gravitational stellar collapses in our galaxy

117 (LVD Collaboration, 1992; 2005). It is well known that there is a rather remarkable correlation

118 between the background signal of these detectors and the alpha decays due to ^{222}Rn (e.g., Bruno and

119 Meghetti, 2006). In addition, we will present some the data of an experiment on radon monitoring

120 in the area that recorded the effects of few aftershocks with $M_L>3$.

121

122 **Methods**

123 Details on the type and functioning of LVD detector are extensively given in LVD Collaboration

124 (1992; 2005). Here, we summarize the main technical features and principles (cf. also Anzivino et

125 al., 1993 for details on the electronics).

126 Single LVD detectors consist of an active scintillator mass of 1000 t constructed in stainless still

127 counters (1.5 m^3 each in volume, with walls of 4 mm thick). Currently an array of 840 scintillators

128 is deployed in a compact and modular geometry. Additionally, counters are shielded by iron layers

129 from 1.5 cm to 2 cm in thickness. Neutrinos detections occurs by counting the inverse beta decay

130 reaction of electron anti-neutrinos on scintillator protons followed by the neutron capture. External

131 counters (43%) operate at energy threshold Eh ~ 7 MeV, whereas the inner ones (57%) run at Eh ~4

132 MeV and are better shielded from rock radioactivity. Counters are equipped with an additional

133 refinement channel, set at a lower threshold El ~ 0.8 MeV to record γ pulses. Thus, every ten

134 minutes the low threshold counting rate of each counter is activated (within a time window of 10

135 seconds) to measure the background at the low energy threshold. This background is essentially

136 related to the nuclear decays of ^{238}U, ^{232}Th and ^{40}K present in the surrounding rocks and

environmental radon; secondary neutral particles generated in muon interaction with the rocks or within detector's materials may also contribute to background levels. Recently, Bruno and Menghetti (2006) concentrated their work on low energy signals and found a remarkable correlation between the LVD counting rates and those obtained by a alpha particles radon-meter (with a relative error of about 10% at 95% confidence levels) (Fig. 2). In particular, they retrieved a linear relationship of this type, for LVD counts being comprised between 40 and 75

$$C_{Rn}\left[Bq/m^3\right] = 7LVD_{cts} - 290 \qquad (1)$$

so that, within this range, a 1 count/sec step measured at LVD is roughly equivalent to a 7 Bq/m^3 in terms of radon activity. They pointed out that there is a time delay between the LVD data and those of radon due to the higher efficiency of γ counts in respect to the α counts associated with the radon decay chain. Moreover, they showed that the opening of the Gran Sasso National Laboratories during working hours modulates concordantly the LVD and the radon signal due to air ventilation, leading to daily fluctuations up to about 200 Hz (cf. Fig. 2). These effects in tunnels and underground openings have been also described by Richon et al. (2009) and Eff-Darwich et al. (2002; 2008). Obviously these fluctuations may somehow effect the peak geometry of the recorded timeseries. Previous works on radon emissions within these laboratories were performed by Plastino and Bella (2001), Plastino et al. (2009).

Fig. 2

We installed three automatic radon monitoring stations at selected sites along the NE-SW Appenine major faults by utilizing three DOSEman electronic radon sensors (produced by SARAD Gmbh). One was deployed along the Paganica fracture, one at the Capannelle Pass and the third was located near the village of Aringo, at about 25 km NNE of L'Aquila (see Fig. 3).

163

164   **Fig. 3**

165

166   In these detectors, the radon gas diffuses through a leather membrane into a cylindrical

167   measurement chamber (12 cm^3 in volume); here the charged alpha particles interact with a Si-doped

168   semiconductor detector and are counted by an automated electronic spectrometer. The counts are

169   stored and instantaneously processed by a multichannel analyser that splits them into discrete

170   energetic domains, known as Regions of Interest (ROIs), thus the spectrum of the radon and its

171   progeny can be reconstructed (Fig. 4). The sensitivity of these detectors covers the range 10 Bq/m^3

172   to 4 millions of Bq/m^3.

173   Each single DOSEman detector, used during our experiment, was carefully calibrated within a

174   "radon chamber" to measure the alpha particles within delimited energy windows. In particular, the

175   Paganica station and the Capannelle station measured within 4410-9555 keV and 4830-9875 keV,

176   respectively, whereas the Aringo station was measuring between 4620-9765 keV (Fig. 4). These

177   windows include the peaks of ^{222}Rn and its progeny (^{218}Po, ^{214}Po) together with ^{220}Rn, thoron (the

178   latter related to the decay of the ^{232}Th chain). However, Gründel and Postendörfer (2003; p. 290)

179   emphasized that the counts for ^{214}Po need to be corrected due to the fact that the higher side of the

180   ^{220}Rn spectrum somehow overlaps the ^{214}Po peak. Thus, they suggested that 7.5 % of the counts of

181   the latter may be due to thoron.

182

183   **Fig. 4**

184

185   Appropriate radon activities in Bq/m^3 can be computed from the total counts of single ROIs (within

186   a given sampling-time: 6 hours in our case) by means of the following relationship (Streil et al.,

187   2002; Gründel and Postendörfer, 2003):

188     $$C_i \left[\text{Bq/m}^3 \right] = \left(C_{f_i} / Cts * \left(1/t_s \right) \right) * 1000 \qquad (2)$$

7

189 where C_{fi} is calibration factor of the instrument (linked to the chamber volume) Cts are the counts, t_s

190 is the sampling time (in minutes) and 1000 is the conversion factor from kBq/m^3 to Bq/m^3. Radon

191 can be computed in *fast mode* counting ^{222}Rn and ^{218}Po only, or *slow mode* that includes the counts

192 of ^{214}Po as well. The reported data were obtained by utilizing the "fast mode" option since ^{214}Po

193 may combine with resident moisture particles, plus we don't have to take into account thoron

194 interferences (on the ^{214}Po peaks). The new generation of DOSEman detectors have instrumental

195 uncertainties, for radon concentrations at 1,000 Bq/m^3 of about 10%, drastically decreasing at

196 higher emissions. We also included, within the Paganica station a temperature data logger (Testo

197 905-T2) to record the soil temperatures a with sample time of 1 hour, since this parameter is crucial

198 in better interpreting the radon signal (Iskandar et al., 2004).

199 Earlier studies (Bellotti et al., 2007) have shown that in the Abruzzo region there are no particular

200 risks regarding the presence of radiogenic rocks and/or soils. Indoor measurements average 60

201 Bq/m^3, whereas peak values have only been recorded in the central part of l'Aquila province (up to

202 about 1100 Bq/m^3). Systematic soil measurements give mean ^{238}U concentrations of 2.5 ppm (Sarra

203 et al., 2012) with radon concentrations approaching 25 Bq/kg, under the assumption that secular

204 equilibrium conditions are reached (Parks et al., 2013).

205

206 **LVD data during early-mid stages of the l'Aquila seismic sequence**

207 We hereby present and analyze the LVD data collected from March 2 to May 1, 2009 at the Gran

208 Sasso National Laboratories near the village of Assergi, located at 15 km NE of l'Aquila (Fig. 5).

209 Then we compare some of our data with LVD traces during the aftershocks that occurred during our

210 monitoring experiment. We have also included the timeseries of events with $M_L>2$ as well as the

211 histograms of the total number of earthquakes (above the cited reference magnitude) during the

212 evolution of the seismic swarm. More reliable LVD data are those evidence by gray bands that refer

213 to the weekly closure of the laboratories. Among these we have those of March 28-30 and April 4-5

214 that preceded the mainshock of April 6. It can be easily seen that there is no clear peak in LVD

counts prior the foreshocks of March 30, with two events reaching a magnitude M_L of about 4.

Similarly, the peak that preceded the major earthquake of April 6 reaches a value of 50 counts and its height is minor in comparison of the fluctuations present in the whole dataset. However, after the mainshock there is an increase in LVD counts that reach 55 counts/sec. The major aftershocks (of April 7 and April 9, with ML 5.3 and ML 5.4, respectively) occur during a descending trend in LVD counts. During this span of time the labs were obviously closed for safety reasons. In this period the signal is more stable than earlier and increase to 58 counts by April 11 likely due to the enhanced fracturing associated with the aftershocks. Then a decreasing trend is recorded with one discontinuity on April 14 followed by a relatively stable signal until the sharp increase (but relatively low in counts: 52) during the early hours of April 19 which is not accompanied or followed by any significant seismic event, and the number of earthquakes falls below 5 per day. A nearly similar peak (in counts) occurs during the evening of April 22 (53 counts/sec) and precede the two events of April 23 with $M_L > 4$. The major peak of April 27 is not correlated with any M_L 3-4 event and is probably associated with an increase in microseismicity. Finally the peak of May 1 seems to be postseismic to the 3.8 M_L event and a moderate increase in the number of earthquakes.

Fig. 5

Radon measurements during the mid stages of the l'Aquila seismic sequence

In Fig. 6 we report the data collected during our experiment at three selected sites. One was located along the Paganica fracture that runs parallel to the regional NE-SW faulting system, one at the Capannelle pass and the third was located near the village of Aringo, i.e. the northeastern edge of our prospecting area.

The Paganica station was deployed at about 3 km NW of the village just below the soil-rock interface (at a depth of about 70 cm) that separates the colluvium deposits from the upper Cretaceous calcarenites and breccias that outcrop in the area. The Capannelle station was inserted

241   into the thick colluvium soil (at a depth of 1 m) that overlays the lower Cretaceous limestones of the

242   "Maiolica" Formation. Finally, the Aringo station was inserted at a depth of 1m in the colluvium

243   soil that covers the upper Miocene sandstones and mudstones ("Flysch della Laga"), at a distance of

244   about 2 km, NW of the village of Aringo.

245   The Paganica station shows an overall increasing trend in radon emissions reaching 830 Bq/m^3 and

246   an average of 600 ± 350 Bq/m^3 during the exposure time. In this section we simply compare these

247   measurements with those obtained at the other two sites, and will be better describe the timeseries

248   recorded at Paganica in the following section.

249   The radon signal at Capannelle station is more fluctuating in terms of radon concentration an we

250   may easily recognize two periods with higher ^{222}Rn emissions. The first one, of April 24 2009 being

251   postseismic to an event of magnitude $M_L=4$, with radon reaching 1100 Bq/m^3. Then radon

252   concentrations moderately decrease and fluctuate nearly above 500 Bq/m^3 until the afternoon of

253   April 26 likely due to the abundance of earthquakes above $M_L>3$ (nine of them were recorded). In

254   the following days the radon signal decreases together with active seismicity. Until April 28 the

255   radon signal is low ~400 Bq/m^3, and we only have 4 earthquakes that reach $M_L= 3$ or slightly

256   higher. It is interesting to note that radon increases after the onset of two events (in the morning of

257   April 28) approaching to M_L~3 (together with a time gap in the release of seismic energy with

258    $M_L>2$) until it reaches a relative maximum up to 1150 Bq/m^3. Then the signal moderately decreases

259   during April 29 when the total amounts of event has only a moderate increase (from 100 to 130 per

260   day). Moreover, there are no particular peaks before the seismic event of May 1, that reaches a

261   magnitude $M_L=3.8$.

262

263   **Fig. 6**

264

265   Finally the radon signal for the Aringo station is somehow higher in terms of radon concentration

266   being up to 1600 Bq/m^3, with an average of 1000 ± 150 Bq/m^3. In this case the signal is rather noisy

267   and fluctuating and there is no apparent correlation with active seismicity. This is probably due to

268   the thick colluvium cover and the nature of the basement rocks that attenuated the vibrations

269   associated with seismic transients. It is not excluded that the irregular topography in the

270   surroundings of the station made this site more vulnerable to the effects of environmental

271   parameters.

272

273   **Fig. 7**

274

275   **Insights on radon emissions at the Paganica Station**

276   We hereby report the full data set recorded at the Paganica station which seems to be more reliable

277   due to the fact that was inserted within the bedrock just below the soil-rock interface and seems to

278   better respond to seismic shaking (e.g., Perrier et al., 2013). This has also been operative for a

279   longer time essentially for logistic reasons. In particular, this station has been deployed directly onto

280   the fracture zone whose activation caused the major damages in the nearby village during the

281   mainshock of April 6, 2009. The reported timeseries (Fig. 7) show a rather persistent increase in

282   radon emissions that fluctuate around mean values. Fluctuation in the signal seem to be related to

283   changes in environmental parameters, such as soil and air temperatures and atmospheric pressure

284   that affect radon transfer toward the surface. Meteorological data were acquired, as daily averages,

285   from the metereological station at Ponte San Giovanni (Fig. 8). In Table 2 we report the correlation

286   coefficients between the daily averages of radon emissions and the environmental parameters (soil

287   and air temperatures, atmospheric pressures, air humidity and rain).

288

289   **Fig. 8 and Table 2**

290

291   Conversely to what observed in volcanic areas (such as Stromboli and Etna, cf. Laiolo et al., 2012;

292   Morelli et al., 2006), here we have a positive correlation of radon emissions with increasing soil and

11

293   air temperatures. This peculiarity was already observed, since temperature may affect the emanation

294   factor of radon from under laying rocks (Iskandar et al., 2004; Girault et al., 2011), thus giving

295   higher radon emissions (cf. Finkelstein et al., 2006).

296   Increasing radon concentrations occur more clearly since May 5, 2009, being essentially correlated

297   with a progressively higher number of daily earthquakes. This is also proved by the Multiple Linear

298   Regression Analysis used to graphically minimize the effects of the cited environmental parameters

299   on the raw radon signal (cf. Laiolo et al., 2012). The results indicate the influence of temperature

300   with the residuals of radon emissions, whereas other environmental parameters do not particularly

301   affect the cited signal (cf. Table 2).

302

303   **Fig. 9**

304

305   However, the trend of the residuals, reported in Fig. 9, still maintains rather visible fluctuations.

306   To have a better picture of these variations we used a graph that reports the time series of the

307   residuals compared with the magnitude of aftershocks with $M_L > 2$ that occurred during the time

308   span of our experiment (Fig. 10). Major variations occur on May 1, being essentially coseismic with

309   the onset of an aftershock of $M_L = 3.8$ (at 5:12 GMT) when ^{222}Rn drops down to 260 Bq/m^3 .

310   Another drastic variation is the one that precedes of about 12 hours the event of May 14, 2009 (at

311   6:30 GMT) that shows a similar magnitude and radon reaches a relative maximum of 1220 Bq/m^3.

312   The epicentral distance of the above earthquakes was respectively 3 and 18 km (a sketch of

313   aftershocks location is shown in Fig. 11). It is interesting to point out that the latter aftershock is the

314   only one that shows, within the span of time of our monitoring, a focal mechanism of a typical *pure*

315   *normal fault*. All other earthquakes show oblique components due to shearing.

316

317   **Fig. 10 and Fig. 11**

318

319   In general, fluctuation of the radon signal do not seem to be correlated with other particular seismic

320   events of lower magnitude.

321

322   **Discussion and conclusions**

323   The Aquila seismic sequence has demonstrated the limits of the potential role of radon as

324   earthquake precursor, particularly if radon emissions are monitored at single sites without taking

325   into account the local geology. With no doubt radon anomalies may be precursors of major seismic

326   events but may also be coseismic, postseismic and/or related to microseismicity (cf., Reddy et al.,

327   2004). However, this has been a rather debated issue in recent years (e.g., Wyss, 1991; 1997;

328   Wakita, 1996; Nature debates, 1999; Planinić et al., 2004; Zmazek et al., 2005; Immè and Morelli,

329   2012). In particular, Planinić et al. (2001) and Zmazek et al. (2005) have discussed the limits of

330   some assumptions at the base of some empirical relationships that correlated radon emissions with

331   the earthquake magnitudes (e.g., Dobrovolsky et al., 1979) without considering the effects of

332   environmental parameters.

333   In particular, the analysis of the LVD signal has shown that low-energy measurements can be used

334   essentially for assessing the radon background within the Gran Sasso National Laboratories

335   (essentially oriented in evaluating the radon exposure of personnel and related health standards). In

336   fact, there is no evidence of diagnostic peaks in LVD counts before and during the Aquila

337   mainshock of April 6, 2009. However, after this event there is a moderate increase in LVD counts,

338   but major aftershocks (of April 7 and April 9, with M_L 5.3 and M_L 5.4) take place during a

339   decreasing trend in the counts themselves. The reason for these discrepancies are essentially

340   intrinsic to the architectural geometry of tunnels and "chambers" of the laboratories. In particular,

341   the LVD measurements site is within a major hall where the floor is covered by a thick concrete

342   pavement. Moreover, the site is affected by enhanced ventilation during working days and the doors

343   connected with the tunnels are opened rather continuously. An additional issue, strictly geologic, is

344   that the LVD site is not laying onto a regional fault that was activated during the seismic crisis. We

13

345 may thus conclude that LVD measurements are nor reliable to assess precursory signals related to

346 radon prior and during the occurrence of a seismic sequence.

347 However, the data collected during our experiment have more complex radon signatures. First, the

348 measuring stations were deployed at a rather low depth (0.7-1 m) and therefore the signal was not

349 stable due to the effects of environmental parameters. However, the radon signal at the Paganica

350 station seems to be more reliable. The reason for its higher efficiency in recording radon variations,

351 before and during seismic aftershocks, seems to be related to the fact that the station was set within

352 the bedrock itself (Upper Cretaceous calcarenites and breccias) that was affected by a major fault

353 actively displaced during the onset of the mainshock.

354 The other two measuring stations were inserted into thicker colluvial soils that cover bedrock

355 formations and, in this case also, were deployed onto fracture systems that run parallel to the major

356 faults trending NE-SW. In spite of this, the less efficient was the one that inserted into the soil that

357 covers the "softer" arenaceous marls of Flysch della Laga formation. This seems to support the idea

358 that the nature of bedrocks coupled with the position of the radon detector may somehow effect the

359 radon signals which appear, in the latter cases, to be more noisy and randomly fluctuating, thus

360 masking the possible effects of local seismicity (cf. Perrier et al., 2013).

361 In conclusion, our experiment indicates that particular attention should be given to the choice of the

362 sites for radon measurements. Thus, radon monitoring in seismogenic areas should be undertaken

363 only by measuring the radon signals at sites that are effectively located onto major tectonic

364 structures. In deploying stations we should make sure that the detectors are preferentially placed

365 directly into bedrock units (particularly if these consist of massive rocks that are not radiogenic).

366 Insertion of radon sensors at higher depths could help in minimizing the effects of environmental

367 parameters on the radon signal. Moreover, in placing the measuring stations we should avoid sites

368 where there is a fluctuation of the water bed that may modulate and disturb the radon signal.

369 In conclusion, we believe that a network for automatic radon measurements opportunely installed

370 could be a starting point for monitoring regional seismicity (Crockett et al., 2006; Papastefanou,

371   2010). Statistical and more reliable results could be accepted only after few years of continuous

372   measurements along active faults. This would give us a better clue to understand their dynamic

373   behavior, in space and time, before, during and after the onset and development of a seismic crisis.

374

384
385
386   **References**

387

388   Akinci A., Galadini F., Pantosti D., Petersen M., Malagnini L., Perkins D., 2009. Effect of Time

389   Dependence on Probabilistic Seismic-Hazard Maps and Deaggregation for the Central Apennines,

390   Italy. Bulletin of the Seismological Society of America April 2009 vol. 99 no. 2A, 585-610, doi:

391   10.1785/0120080053.

392

393   Alparone, S., Behncke, B., Giammanco, S., Neri, M., Privitera, E., 2005. Paroxysmal summit

394   activity at Mt. Etna (Italy) monitored through continuous soil radon measurement. Geophysical

395   Research Letters 2: L16307, doi:10.1029/2005GL023352.

396

397   Amato, A., Galli, P., Mucciarelli, M., 2011. Introducing the special issue on the 2009 L'Aquila

398   earthquake. Bollettino di Geofisica Teorica ed Applicata 52 (3), 357-365.

399

400 Anzivino, G., Benvenuto, P., Bianco, S., Casaccia, R., Dulach, B., Fabbri, D., Fabbri, F.L., Gatta,

401 M., Giardoni, M., Laakso, I., Lindozzi, M., Passamonti, L., Russo, V., Sarwar, S., Sensolini, G.,

402 Ventura, M., Votano, L., Zallo, A., Mencarini, D., Pallante, E., Aftab, Z., Ali, M.M., Chen, K.,

403 Chen, R., Cong, S., Cui, X., Ding, H., Gao, B., Li, Y., Lu, L., Minhas, B.K., Shi, Z., Shah, A.R.,

404 Sun, Y., Zhou, X., 1993. The LVD tracking system chamber. Nuclear Instruments and Methods in

405 Physics Research A 329, 521-540.

406

407 Bellotti, E., Di Carlo, G., Di Sabatino, D., Ferrari, N., Laubenstein, M., Pandola, L., Tomei, C.

408 2007. γ-ray spectrometry of soil samples from the Provincia dell'Aquila (Central Italy). Applied

409 Radiation and Isotopes 65 (7), 858-865.

410

411 Biagi, P. F., Castellana, L., Maggipinto, T., Loiacono, D., Schiavulli, L., Ligonzo, T., Fiore, M.,

412 Suciu, E., Ermini, A., 2009. A pre seismic radio anomaly revealed in the area where the Abruzzo

413 earthquake (M=6.3) occurred on 6 April 2009. Natural Hazards Earth System Sciences 9, 1551-

414 1556, doi:10.5194/nhess-9-1551-2009.

415

416 Bonfanti, P., Genzano, N., Heinicke, J., Italiano, F., Martinelli, G., Pergola, N., Telesca, L.,

417 Tramutoli, V. 2012. Evidence of CO_2-gas emission variations in the central Apennines (Italy)

418 during the L'Aquila seismic sequence (March-April 2009). Bollettino di Geofisica Teorica ed

419 Applicata 53 (1), 147-168.

420

421 Bruno G., Menghetti H., 2006. Low energy background measurement ($\sim$ 0.8 MeV) with the LVD.

422 Journal of Physics Conference Series 39, 278–280.

423 Burton, M., Neri, M., Condarelli, D., 2004. High spatial resolution radon measurements reveal

424 hidden active faults on Mt. Etna. Geophysical Research Letters 31 (7), L07618.

425

426 Cafagna, F., 2007. Misure di emissioni di radon in diversi contesti geodinamici: i casi del Gran

427 Sasso e di Stromboli. Tesi di Laurea Magistralis in Scienze Geologiche, Dipartimento di Scienze

428 Mineralogiche e Petrologiche, Università degli Studi di Torino, pp. 265.

429

430 Cartlidge, E., 2014. Human Activity May Have Triggered Fatal Italian Earthquakes (Emilia), Panel

431 says. Science, 344 no. 6180, 141. doi: 10.1126/science.344.6180.141.

432

433 Cafagna, F., 2007. Misure di emissioni di radon in diversi contesti geodinamici: i casi del Gran

434 Sasso e di Stromboli. Tesi di Laurea Magistralis in Scienze Geologiche, Dipartimento di Scienze

435 Mineralogiche e Petrologiche, Università degli Studi di Torino, 265 pp.

436

437 Chiaraluce,, L., Chiarabba C., De Gori, P., Di Stefano, R., Improta, L., Piccinini, D., Schlagenhauf,

438 A., Traversa, P., Valoroso, L., Voisin, C., 2011. The 2009 L'Aquila (central Italy) seismic

439 sequence. Bollettino di Geofisica Teorica ed Applicata 52 (3), 367-387

440

441 Chiodini, G., Caliro, S., Cardellini, C., Frondini, F., Inguaggiato, S., Matteucci, F., 2011.

442 Geochemical evidence for and characterization of CO_2 rich gas sources in the epicentral area of the

443 Abruzzo 2009 earthquakes. Earth and Planetary Science Letters 304 (3–4), 389–398.

444

445 Chirkov, A.M., 1975. Radon as a possible criterion for predicting eruptions as observed at

446 Karymsky volcano. Bulletin of Volcanology 39, 126-131.

447

448 Cicerone, R.D., Ebel, J.E., Britton, J., 2009. A systematic compilation of earthquake precursors.

449 Tectonophysics 476 (3-4), 371-396.

450

451 Cigolini, C., Salierno, G., Gervino, G., Bergese, P., Marino, C., Russo, M., Prati, P., Ariola, V.,

452 Bonetti, R., Begnini, S., 2001. High-resolution Radon Monitoring and Hydrodynamics at Mount

453 Vesuvius. Geophysical Research Letters 28 (21), 4035-4039.

454

455 Cigolini, C., Gervino, G., Bonetti, R., Conte, F., Laiolo, M., Coppola, D., Manzoni, A., 2005.

456 Tracking precursors and degassing by radon monitoring during major eruptions at Stromboli

457 Volcano (Aeolian Islands, Italy). Geophysical Research Letters 32, L12308

458 doi:10.1029/2005GL022606.

459

460 Cigolini, C., Laiolo, M., Coppola, D., 2007. Earthquake-volcano interactions detected from radon

461 degassing at Stromboli (Italy). Earth and Planetary Science Letters 257, 511-525.

462

463   Cigolini, C., Poggi, P., Ripepe, M., Laiolo, M., Ciamberlini, C., Delle Donne, D., Ulivieri, G.,

464   Coppola, D., Lacanna, G., Marchetti, E., Piscopo, D., Genco, R., 2009. Radon surveys and real-time

465   monitoring at Stromboli volcano: influence of soil temperature, atmospheric pressure and tidal

466   forces on 222Rn degassing. Journal of Volcanology and Geothermal Research 184(3-4), 381-388.

467

468   Cigolini, C., 2010. The dynamics of a double-cell hydrothermal system in triggering seismicity at

469   Somma-Vesuvius: results from a high-resolution radon survey (revisited). Bulletin of Volcanology

470   72, 693–704.

471

472   Cigolini C., Laiolo, M., Ulivieri, G., Coppola, D., Ripepe, M., 2013. Radon mapping, automatic

473   measurements and extremely high 222Rn emissions during the 2002–2007 eruptive scenarios at

474   Stromboli volcano. Journal of Volcanology and Geothermal Research 264, 49- 65.

475

476   Connors, C., Hill, B., La Femina, P., Navarro, M., Conway, M., 1996. Soil Rn-222 pulse during the

477   initial phase of the June August 1995 eruption of Cerro Negro, Nicaragua. Journal of Volcanology

478   and Geothermal Research 73, 119-127.

479

480   Cox, M.E., 1980. Ground Radon Survey of a Geothermal area in Hawaii. Geophysical Research

481   Letters 7, 283-286.

482

483   Crockett, R.G.M., Gillmore, G.K., Phillips, P.S., Denman, A.R., Groves-Kirkby, C.J., 2006. Radon

484   anomalies preceding earthquakes which occurred in the UK, in summer and autumn 2002. Science

485   of the Total Environment 364 (1–3), 138-148.

486

487   De Martini, P., Cinti, F., Cucci, L., Smedile, A., Pinzi, S., Brunori, C., Molisso, F., 2012. Sand

488   volcanoes induced by the April 6th 2009 Mw 6.3 L'Aquila earthquake: a case study from the Fossa

489   area. Italian Journal of Geosciences 131 (3), 410-422. doi: 10.3301/IJG.2012.14.

490

491   Di Luccio, F., Ventura, G., Di Giovambattista, R., Piscini, A., Cinti, F.R., 2010. Normal faults and

492   thrusts re-activated by deep fluids: the 6 April 2009 Mw 6.3 L'Aquila earthquake, central Italy.

493   Journal of Geophysical Research 115, B06315. doi: 10.1029/2009JB007190.

494

495   Dobrovolsky, I.P., Zubkov, S.I., Miachkin, V.I., 1979. Estimation of the size of earthquake

496   preparation zones. Pure and Applied Geophysics 117 (5), 1025-1044.

497   Dueñas, C., Fernández, M.C., Carretero, J., Liger, E., Pérez, M., 1997. Release of 222Rn from some
498   soils. Annales Geophysicae 15, 124-133.
499
500   Eff-Darwich, A., Martín, C, Quesada, M., de la Nuez, J., Coello, J., 2002. Variations on the
501   concentration of 222R in the subsurface of the volcanic island of Tenerife, Canary Islands.
502   Geophysical Research Letters 29, 2069-2073.
503
504   Eff-Darwich, A., Viñas, R., Soler, V., de la Nuez, J., Quesada, M.L., 2009. Natural air ventilation in
505   underground galleries as a tool to increase radon sampling volumes for geologic monitoring,
506   Radiation Measurements 43, 1429-1436.
507
508   Fidani, C., 2010. The earthquake lights (EQL) of the 6 April 2009 Aquila earthquake, in Central
509   Italy. Natural Hazards Earth System Sciences 10, 967-978. doi:10.5194/nhess-10-967-2010.
510
511   Finkelstein, M., Eppelbaum L.V., Price, C., 2006. Analysis of temperature influences on the
512   amplitude frequency characteristics of Rn gas concentration. Journal of Environmental
513   Radioactivity 86, 251–270.
514
515   Fleischer, R.L., Mogro-Campero, A., 1985. Association with subsurface radon changes in Alaska
516   and the Northeastern United States with earthquakes. Geochimica and Cosmochimica Acta 49,
517   1061-1071.
518
519   Genzano, N., Aliano, C., Corrado, R., Filizzola, C., Lisi, M., Mazzeo, G., Paciello, R., Pergola, N.,
520   and Tramutoli, V. 2009. RST analysis of MSG-SEVIRI TIR radiances at the time of the Abruzzo 6
521   April 2009 earthquake. Natural Hazards Earth System Sciences 9, 2073-2084. doi:10.5194/nhess-9-
522   2073-2009.
523
524   Girault, F., Perrier, F., 2011. Heterogeneous temperature sensitivity of effective radium
525   concentration from various rock and soil samples. Natural Hazards and Earth System Sciences 11,
526   1619-1626. doi: 10.5194/nhess-11-1619-2011.
527
528   Giuliani, G., 2009. L'Aquila 2009 la mia verità sul terremoto. Castelvecchi Editore, Rome, 166 p.
529

530 Gregori, G.P., Poscolieri, M., Paparo, G., De Simone, S., Rafanelli, C., and Ventrice, G. 2010.
531 "Storms of crustal stress" and AE earthquake precursors. Natural Hazards and Earth System
532 Sciences 10, 319-337, doi: 10.5194/nhess-10-319-2010.

534 Ghosh, D., Deb, A., Sengupta, R., 2009. Anomalous radon emission as precursor of earthquake.
535 Journal of Applied Geophysics 69 (2), 67-81.

537 Gründel, M., Postendörfer. J., 2003. Characterization of an electronic Radon gas personal
538 Dosimeter. Radiation Protection Dosimetry 107 (4), 287–292.

540 Herrmann, R.B., Malagnini, L., Munafò, I., 2011. Regional Moment Tensors of the 2009 L'Aquila
541 Earthquake Sequence. Bulletin of the Seismological Society of America 101 (3), 975-993. doi:
542 10.1785/0120100184.

544 Hishimuma, T., Nishikawa, T., Shimoyama, T., Myajima M., Tamagawa, Y., Okabe, S., 1999.
545 Emission of radon and thoron due to the fracture of rock. Il Nuovo Cimento 22 (3-4), 523-527.

547 Igarashi, G.: Saeki, S.: Takahata, N.: Sumikawa, K.: Tasaka, S.: Sasaki, Y., Takahashi, M., Sano,
548 Y., 1995. Ground-water Radon Anomaly before the Kobe Earthquake in Japan. Science 269, 60-61.

550 Immè, G., Morelli, D., 2012. Radon as Earthquake Precursor. In: D'Amico, S., (Eds.), Earthquake
551 Research and Analysis - Statistical Studies, Observations and Planning. InTech Publisher, pp. 143-
552 160. doi: 10.5772/29917 http://www.intechopen.com/books/earthquake-research-and-analysis-
553 statistical-studies-observations-and-planning/radon-as-earthquake-precursor .

555 Iskandar, D., Yamazawa, H., Iida, T., 2004. Quantification of the dependency of radon emanation
556 power on soil temperature. Applied Radiation and Isotopes 60 (6), 971-973.

558 Jordan, T.H., Chen, Y.T., Gasparini, P., Madariaga, R., Main, I., Marzocchi, W., Papadopoulos, G.,
559 Sobolev, G., Yamaoka, K., Zschau, J. 2011. Final report by the International Commission on
560 Earthquake Forecasting for Civil Protection. Operational Earthquake Forecasting: State of
561 Knowledge and Guidelines for Utilization. Annals of Geophysics 54 (4), 315-391. doi: 10.4401/ag-
562 5350.

564 Kawada, Y., Nagahama, H., Omori, Y., Yasuoka, Y., Ishikawa, T., Tokonami, S., and Shinogi, M.,
565 2007. Time-scale invariant changes in atmospheric radon concentration and crustal strain prior to a
566 large earthquake. Nonlinear Processes in Geophysics 14, 123–130. http://www.nonlin-processes-
567 geophys.net/14/123/2007.

568

569 Kumar, A., Singh, S., Mahajan, S., Bajwa, B.S., Kalia, R., Dhar, S. 2009. Earthquake precursory
570 studies in Kangra valley of North West Himalayas, India, with special emphasis on radon emission.
571 Applied Radiation and Isotopes 67, 1904–1911.

572

573 Laiolo, M., Cigolini, C., Coppola, D., Piscopo, D. 2012. Developments in real-time radon
574 monitoring at Stromboli volcano. Journal of Environmental Radioactivity 105, 21- 29.

575

576 Lucente, F.P., de Gori, P., Margheriti, L., Piccinini, D., di Bona, M., Chiarabba, C., Agostinetti,
577 N.P. 2010. Temporal variation of seismic velocity and anisotropy before the 2009 Mw 6.3 L'Aquila
578 earthquake, Italy. Geology 38 (11), 1015-1018.

579

580 LVD Collaboration, 1992. Il Nuovo Cimento A 105, 1793 p.

581

582 LVD Collaboration, 2005. Proc. of the Fifth Int. Workshop on the identification of Dark Matter 471
583 p.

584

585 Mercuri, A., 2009. Terremoti dell'Appenino Centrale e risposta sismica di un generico sito su
586 roccia. Relazioni tra eventi sismici ed emissioni di radon. Tesi di Dottorato in Scienze della Terra
587 (XXI Ciclo). Università degli Studi di Torino, pp. 89.

588

589 Morelli, D., Di Martino, S., Immè, G., La Delfa, S., Lo Nigro, S., Patanè G., 2006. Evidence of soil
590 radon as tracer of magma uprising in Mt. Etna. Radiation Measurements 41(6), 721-725.

591

592 Mogro-Campero, A., Fleischer, R.L., 1977. Subterrestrial fluid convection: a hypothesis for long
593 distance migration of radon within the earth. Earth and Planetary Science Letters 34, 321-325.

594

595 Nature debates, 1999. http://www.nature.com/nature/debates/earthquake/equake_frameset.html

596

597 Ouzounov, D., Freund, F.T., 2004. Mid-infrared emission prior to strong earthquakes analyzed by
598 remote sensing data. Advances in Space Research 33 (3), 268-273.

599

600 Papastefanou, C., 2010. Variation of radon flux along active fault zones in association with
601 earthquake occurrence. Radiation Measurements 45 (8), 943-951.

602

603 Parks, M.M., Caliro, S., Chiodini, G., Pyle, D.M., Mather, T.A., Berlo, K., Edmonds, M., Biggs, J.,
604 Nomikou, P., Raptakis, C., 2013. Distinguishing contributions to diffuse CO2 emissions in volcanic
605 areas from magmatic degassing and thermal decarbonation using soil gas Rn^{222}-delta C^{13}
606 systematics: Application to Santorini volcano, Greece. Earth and Planetary Science Letters 377,
607 180-190.

608

609 Pérez, N.M., Hernández, P.A., Padrón, E., Melián, G., Marrero, R., Padilla, G., Barrancos, J.,
610 Nolasco, D., 2007. Precursory subsurface ^{222}Rn and ^{220}Rn degassing signatures of the 2004 seismic
611 crisis at Tenerife, Canary Islands. Pure and Applied Geophysics 164, 2431-:2448.

612

613 Pergola, N., Aliano, C., Coviello, I., Filizzola, C., Genzano, N., Lacava, T., Lisi, M., Mazzeo, G.,
614 Tramutoli, V., 2010. Using RST approach and EOS-MODIS radiances for monitoring seismically
615 active regions: a study on the 6 April 2009 Abruzzo earthquake. Natural Hazards and Earth System
616 Sciences 10, 239-249. doi: 10.5194/nhess-10-239-2010, 2010.

617

618 Perrier, F., Girault, F., 2013. Harmonic response of soil radon-222 flux and concentration induced
619 by barometric oscillations. Geophysical Journal International 195 (2), 945-971.

620

621 Pinault, J.L., Baubron, J.C., 1996. Signal processing of soil gas radon, atmospheric pressure and
622 soil temperature data: a new approach for radon concentration modeling. Journal of Geophysical
623 Research 101, 3157-3171.

624

625 Planicić, J., Radolić, V., Vuković, B., 2001. Temporal variation of radon in soil related to
626 earthquakes. Applied Radiation and Isotopes 55, 267-272.

627

628 Planicić, J., Radolić, V., Vuković, B., 2004. Radon as an earthquake precursor. Nuclear Instruments
629 and Methods in Physics Research, Section A: Accelerators, Spectrometers, Detectors and
630 Associated Equipment 530 (3), 568-574.
631
632 Plastino, W., Bella, F., 2001. Radon groundwater monitoring at underground laboratories
633 of Gran Sasso (Italy). Geophysical Research Letters 28, 2675–2678.
634
635 Plastino, W., Nisi, S., De Luca, G., Balata, M., Laubenstein, M., Bella, F., 2009. Environmental
636 radioactivity in the ground water at the Gran Sasso National Laboratory (Italy): a possible
637 contribution to the variation of the neutron flux background. Journal of Radioanalytical and Nuclear
638 Chemistry 282 (3), 809-813. doi:10.1007/s10967-009-0151-2.
639
640 Plastino, W., Povinec, P.P., De Luca, G., Doglioni, C., Nisi, S., Ioannucci, L., Balata, M.,
641 Laubenstein, M., Bella, F., Coccia, E., 2010. Uranium groundwater anomalies and L'Aquila
642 earthquake, 6th April 2009 (Italy). Journal of Environmental Radioactivity 101 (1), 45-50.
643
644 Pulinets, S A; Ouzounov, D P; Giuliani, G., Ciraolo, L., Taylor, P.T., 2009. Atmosphere and radon
645 activities observed prior to Abruzzo M6.3 earthquake of April 6, 2009. Eos Trans. AGU 90(52):
646 Abstract AN: U14A-07.
647
648 Reddy, D.V., Sukhija, B.S., Nagabhushanam, P., Kumar, D., 2004. A clear case of radon anomaly
649 associated with a micro-earthquake event in a Stable Continental Region. Geophysical Research
650 Letters 31, L10609. doi: 10.1029/2004GL019971.
651
652 Richon, P., Sabroux, J.C., Halbwachs, M., Vandemeulebrouck, J., Poussielgue, N., Tabbagh, J.,
653 Punongbayan, R., 2003. Radon anomaly in the soil of Taal volcano, the Philippines: a likely
654 precursor of the M 7.1 Mindoro earthquake (1994). Geophysical Research Letters 30 (9), 34-41.
655 doi: 10.1029/2003GL016902.
656
657 Richon, P., Perrier, F., Pili, E., Sabroux, J., 2009. Detectability and significance of 12 hr barometric
658 tide in radon-222 signal, dripwater flow rate, air temperature and carbon dioxide concentration in an
659 underground tunnel. Geophysical Journal International 176 (3), 683-694.
660

661 Riguzzi, F., Crespi, M., Devoti, R., Doglioni, C., Pietrantonio, G., Pisani, A., 2013. Strain rate
662 relaxation of normal and thrust faults in Italy. Geophysical Journal International 195 (2), 815-820.
663 doi: 10.1093/gji/ggt304.

665 Rozhnoi, A., Solovieva, M., Molchanov, O., Schwingenschuh, K., Boudjada, M., Biagi, P. F.,
666 Maggipinto, T., Castellana, L., Ermini, A., Hayakawa, M., 2009. Anomalies in VLF radio signals
667 prior the Abruzzo earthquake (M=6.3) on 6 April 2009, Natural Hazards Earth System Sciences 9,
668 1727-1732. doi: 10.5194/nhess-9-1727-2009, 2009.

670 Sarra, A., Nissi, E., Palermi, S. 2012. Residential radon concentration in the Abruzzo region (Italy):
671 a different perspective for identifying radon prone areas. Environmental and Ecological Statistics,
672 19 (2), 219-247.

674 Scholtz, C.H., Sykes, L.R., Aggarval, Y.P., 1973. Earthquake prediction: a physical basis. Science
675 181, 803-810.

677 Streil, T., Oeser, V., Feige, S., 2002. An electronic radon dosimeter as a multipurpose device-a
678 bridge between dosimetry and monitoring. Geofisica Internacional 41, 285-288.

680 Steinitz, G., Begin, Z.B., Gazit-Yaari, N., 2003. Statistically significant relation between radon flux
681 and weak earthquakes in the Dead Sea rift valley. Geology 31 (6), 505-508.

683 Terakawa, T., Zoporowski, A., Galvan, B., Miller, S.A., 2010. High-pressure fluid at hypocentral
684 depths in the L'Aquila region inferred from earthquake focal mechanisms. Geology 38 (11), 995-
685 998.

687 Thomas, D.M., Cox, M.E., Cuff, K.E., 1986. The association between ground gas radon variations
688 and geologic activity in Hawaii. Journal of Geophysical Research 91, 12186-12198.

690 Toutain, J. P., Baubron, J. C., 1999. Gas geochemistry and seismotectonics: a review.
691 Tectonophysics 304, 1–27.

692

693 Trique, M., Richon, P., Perrier, F., Avouac, J.P., Sabroux, J.C., 1999. Radon emanation and electric
694 potential variations associated with transient deformation near reservoir lakes. Nature 399, 137-141.
695 doi: 10.1038/20161.

696

697 Tuccimei, P., Mollo, S., Vinciguerra, S., Castelluccio, M., Soligo, M., 2010. Radon and thoron
698 emission from lithophysae-rich tuff under increasing deformation: An experimental study.
699 Geophysical Research Letters 37 (5), L05305. DOI: 10.1029/2009GL042134.

700

701 Vaupotiĉ, J., Gregoriĉ, A., Kobal, I., Žvab, P., Kozak, K., Mazur, J., Kochowska, E., Grza☐dziel,
702 D., 2010. Radon concentration in soil gas and radon exhalation rate at the Ravne Fault in NW
703 Slovenia. Natural Hazards and Earth System Science 10 (4), 895-899.

704

705 Wakita H., 1996. Geochemical challenge to earthquake prediction. Proc. Natl. Acad. Sci. USA; 93:
706 3781-3786

707

708 Wyss M. (Ed), 1991. Evaluation of proposed earthquake precursors. Am. Geophys. Union,
709 Washington D.C., 94 pp.

710

711 Wyss M., 1997. Second round of evaluations of earthquake precursors. Pure Appl. Geophys., 149:
712 3-16.

713

714 Zmazek, B., Živčić, M., Todorovski, L., Džeroski, S., Vaupotič, J., Kobal, I., 2005. Radon in soil
715 gas: How to identify anomalies caused by earthquakes. Applied Geochemistry 20 (6), 1106-1119.

716

717

718

719

720

721 **Figure captions**

722

723 Fig. 1. Tectonic setting of the L'Aquila region (a) and earthquake location of the 2009 seismic
724 sequence (for seismic events with $M_L > 2$) (b). The location of the mainshock of April 6, 2009 with
725 M_L 5.9 and those major aftershocks of April 7 and April 9, with magnitudes (M_L) of 5.3 and 5.1
726 respectively, are reported with their focal mechanism solutions (cf. http://cnt.rm.ingv.it/tdmt.html).

727 The mainshock and the second aftershock are related to pure normal faulting whereas the aftershock

728 of April 7 shows an oblique component due to shearing.

729

730 Fig. 2. Comparison between LVD low energy threshold counting rate in s−1 (black) and radon

731 concentrations in Bq/m^3 (gray). Modified after Bruno and Menghetti (2006).

732

733 Fig. 3. Sketch of the location of the radon stations together with the site of Laboratori Nazionali del

734 Gran Sasso (LNGS) where LVD tanks are operative. Metereological data were collected by the

735 station at Ponte S. Giovanni nearby the Scoppito village (http://www.caputfrigoris.it). Locations of

736 single stations were plotted onto a Google Earth image.

737

738 Fig. 4. Total daily decay counts computed by the two DOSEMan alpha-spectrometers (SARAD

739 Gmbh) of the monitoring stations plotted against particles energy (keV), see text for details. PNG:

740 Paganica station, CPNL: Capannelle Pass station, ARG: Aringo station.

741

742 Fig. 5. Large Volume Detector (LVD) low energy traces (~0.8 MeV) collected during the early-mid

743 stages of the seismic sequence compared with earthquakes' magnitude and the daily number of

744 seismic events (with $M_L > 2$). The grey fields indicate the periods when the Laboratories were

745 closed (see text for details).

746

747 Fig. 6. Timeseries of radon emissions (^{222}Rn) collected at monitoring stations during our experiment

748 throughout the mid stages of the l'Aquila seismic sequence compared with the histogram of the

749 total number of seismic events. Sampling time was of 4 hours.

750

751 Fig. 7. Timeseries of radon concentrations at the Paganica Station (a) compared with soil

752 temperature variations (b). The sampling time was 6 hours for both parameters. Red curves

753 represent daily averages.

754

755 Fig. 8. Variation of environmental parameters (atmospheric temperature and pressure, air humidity

756 and rain falls) recorded by the station of Ponte S. Giovanni for the duration of our experiment

757 (http://www.caputfrigoris.it).

758

759 Fig. 9. Timeseries of radon concentrations at the Paganica station and display of the residuals. Data

760 were collected with a sampling time of 6 hours; the thick red curve represent daily smoothing

761   (upper panel). The residuals calculated by means of Multiple Linear Regression (MRL) analysis

762   (i.e., by including the effects of environmental parameters is shown in the lower panel.

763

764   Fig. 10. Comparison of the calculated residuals with the sequence of the aftershocks with $M_L > 2$

765   during the exposure time of our automated detector at the PNG station.

766

767   Fig. 11. Aftershocks locations plotted onto a Google Earth image during the duration of our

768   experiment. Smaller black dots represent the epicentres of events with $M_L < 3$, whereas lighter green

769   circles are aftershocks with $M_L \geq 3$. Focal mechanism solutions for stronger events are also reported

770   (cf. http://cnt.rm.ingv.it/tdmt.html).

Figure 1
Click here to download high resolution image
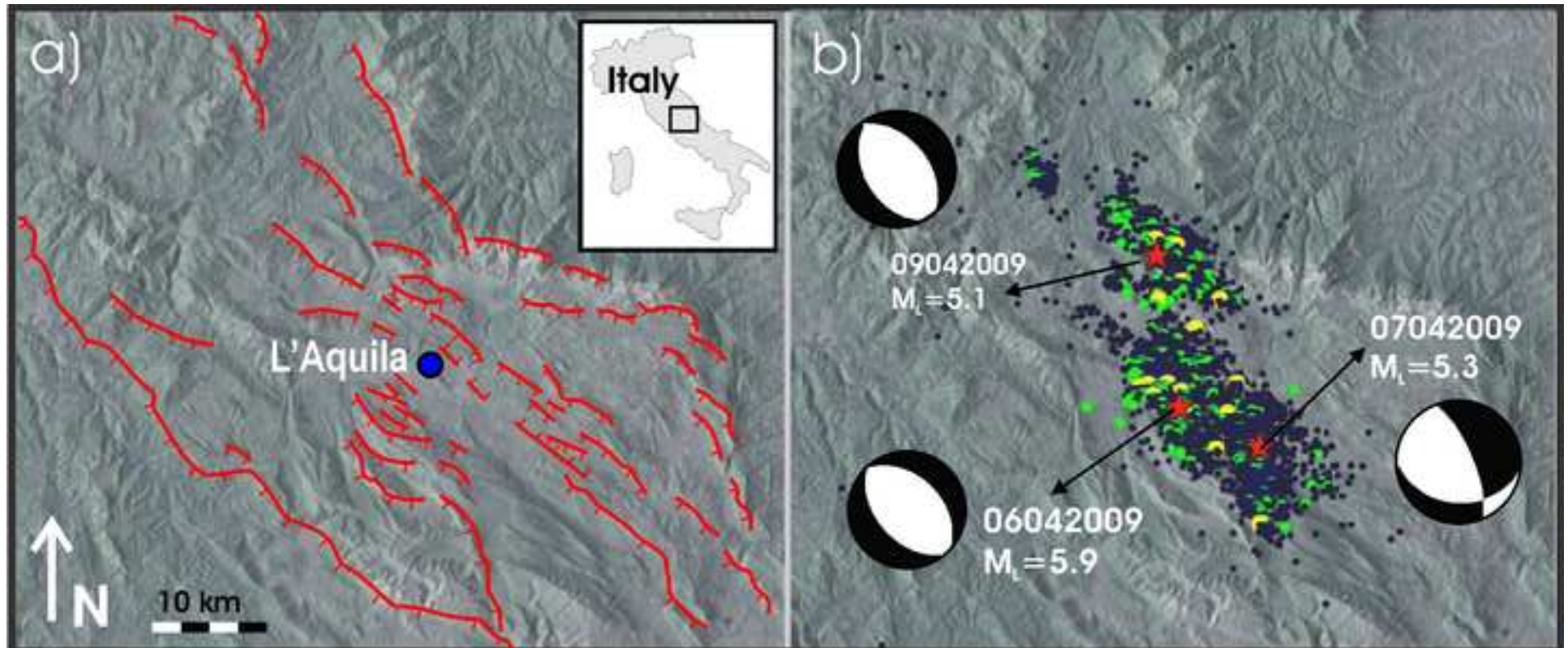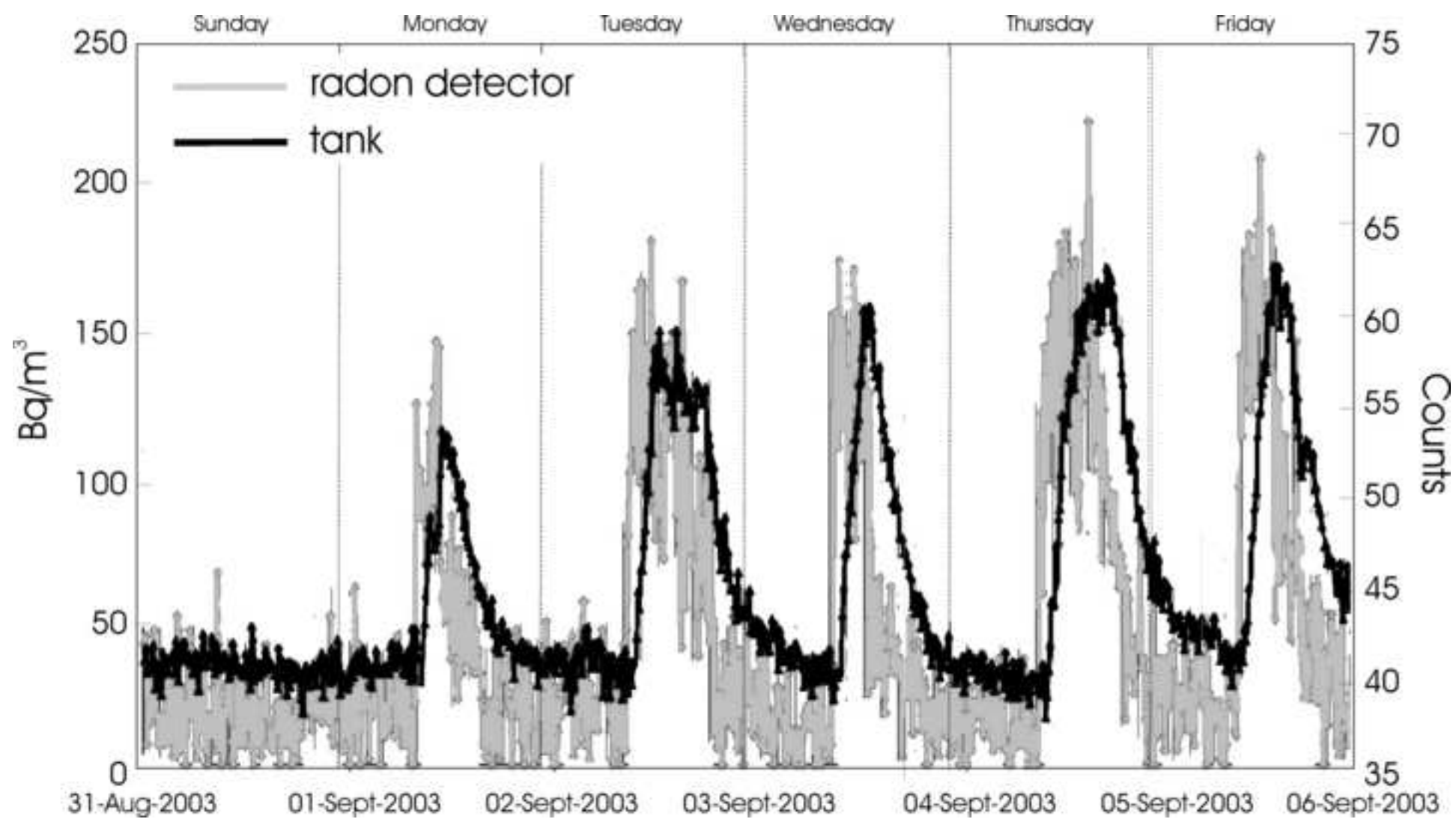
Figure 3
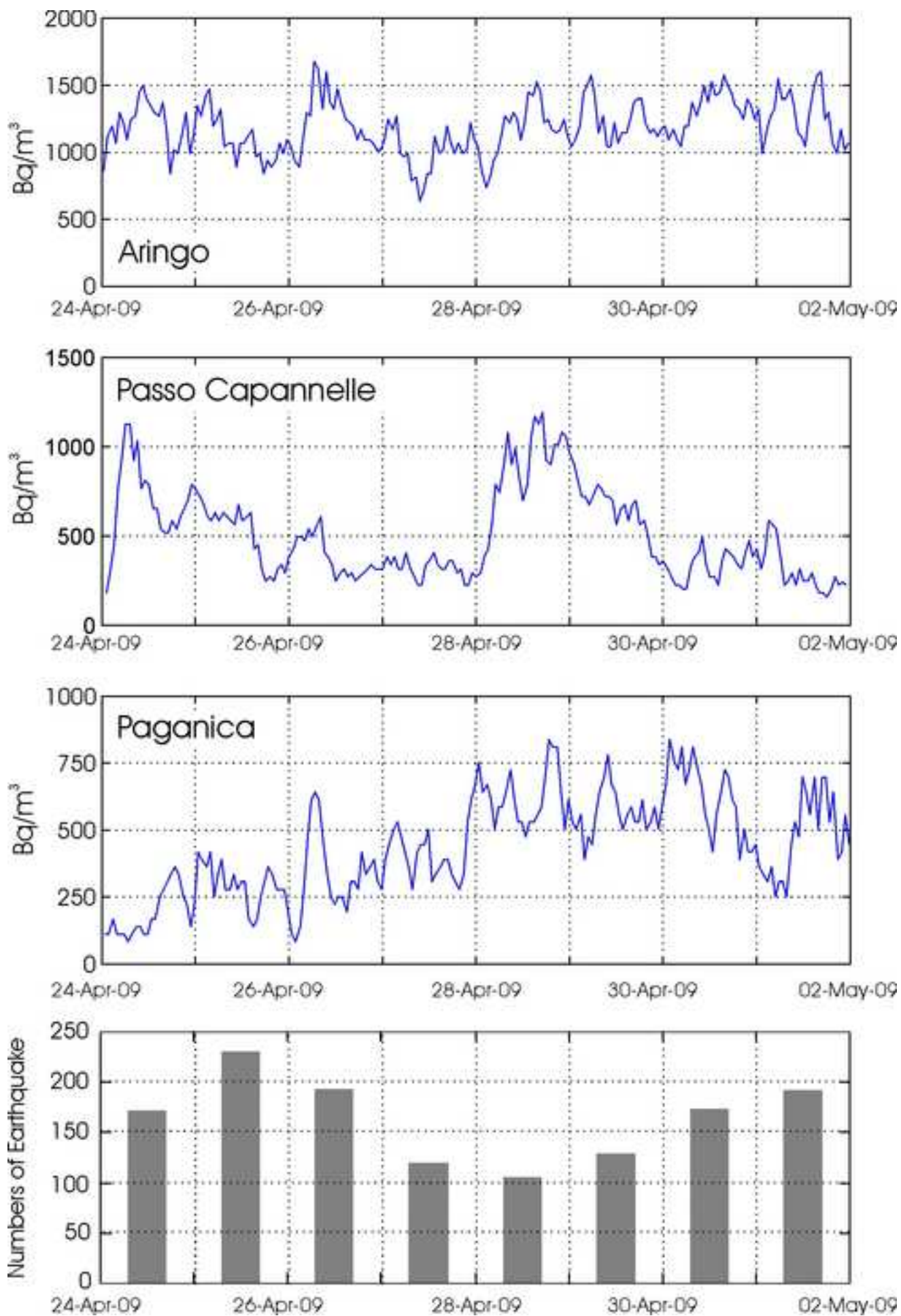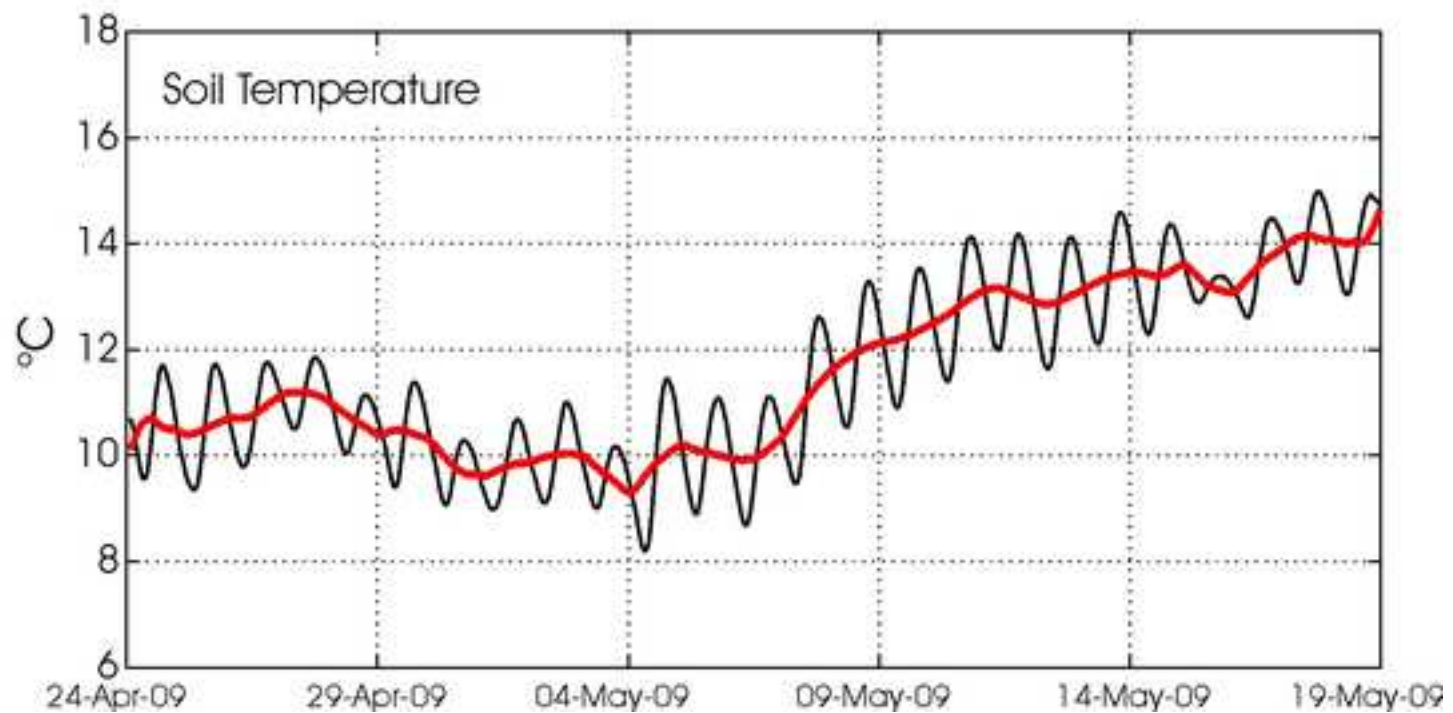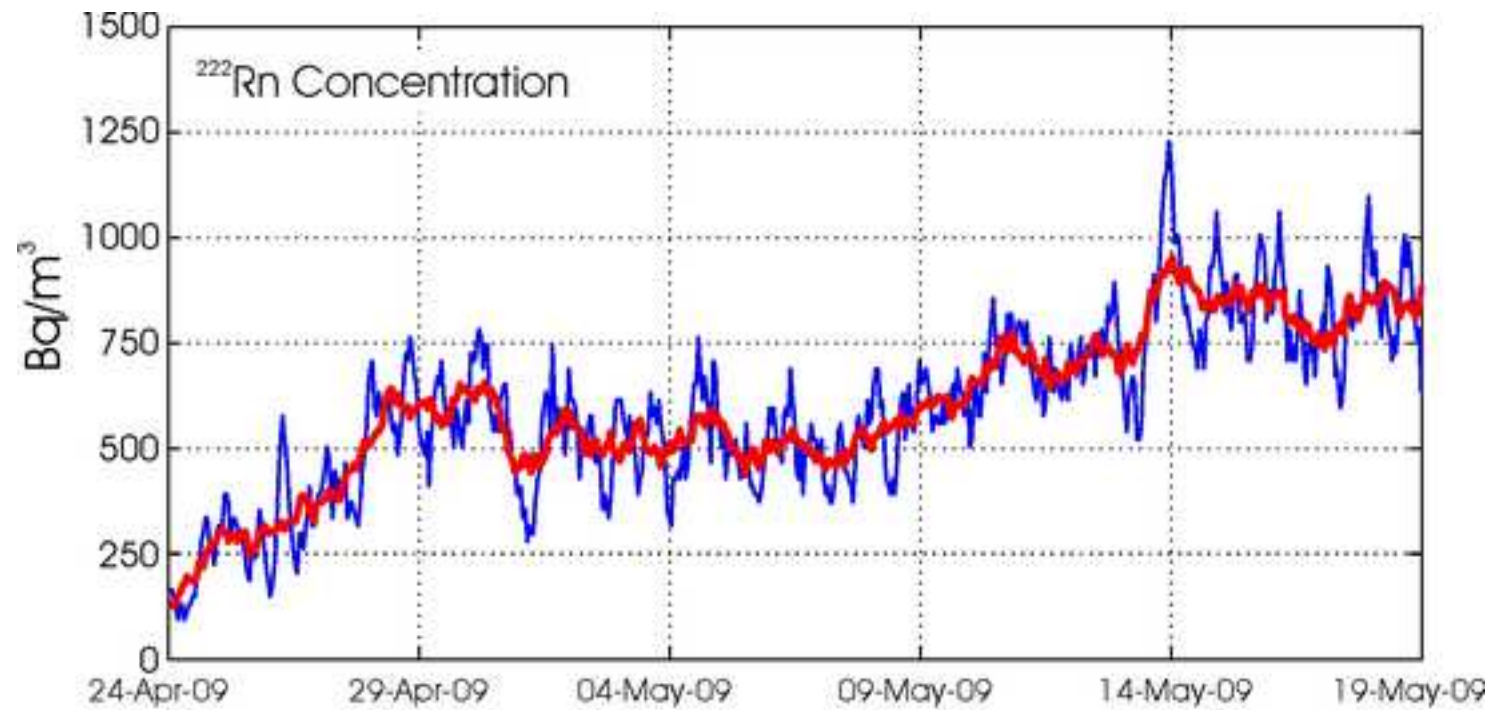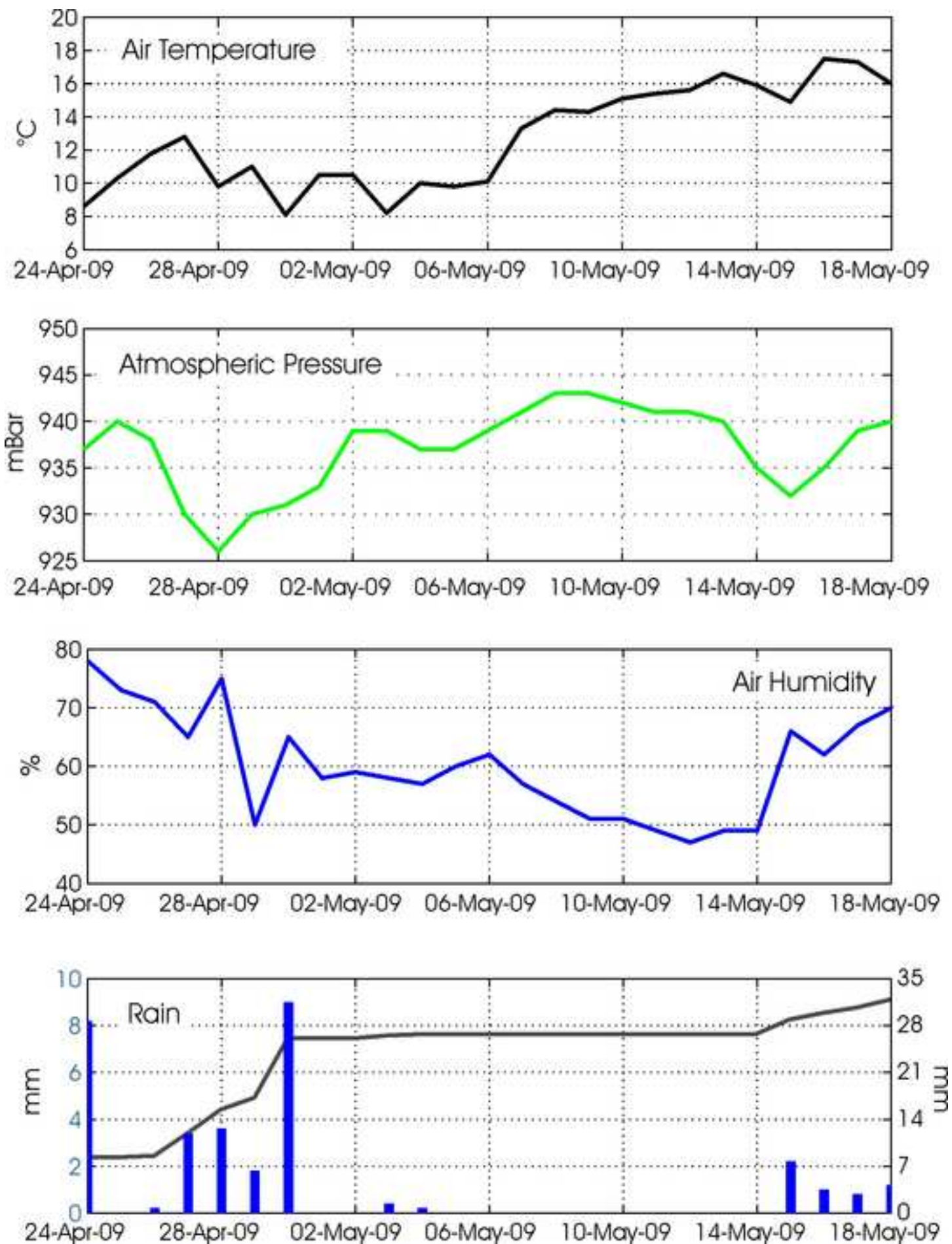**Click here to download high resolution image**
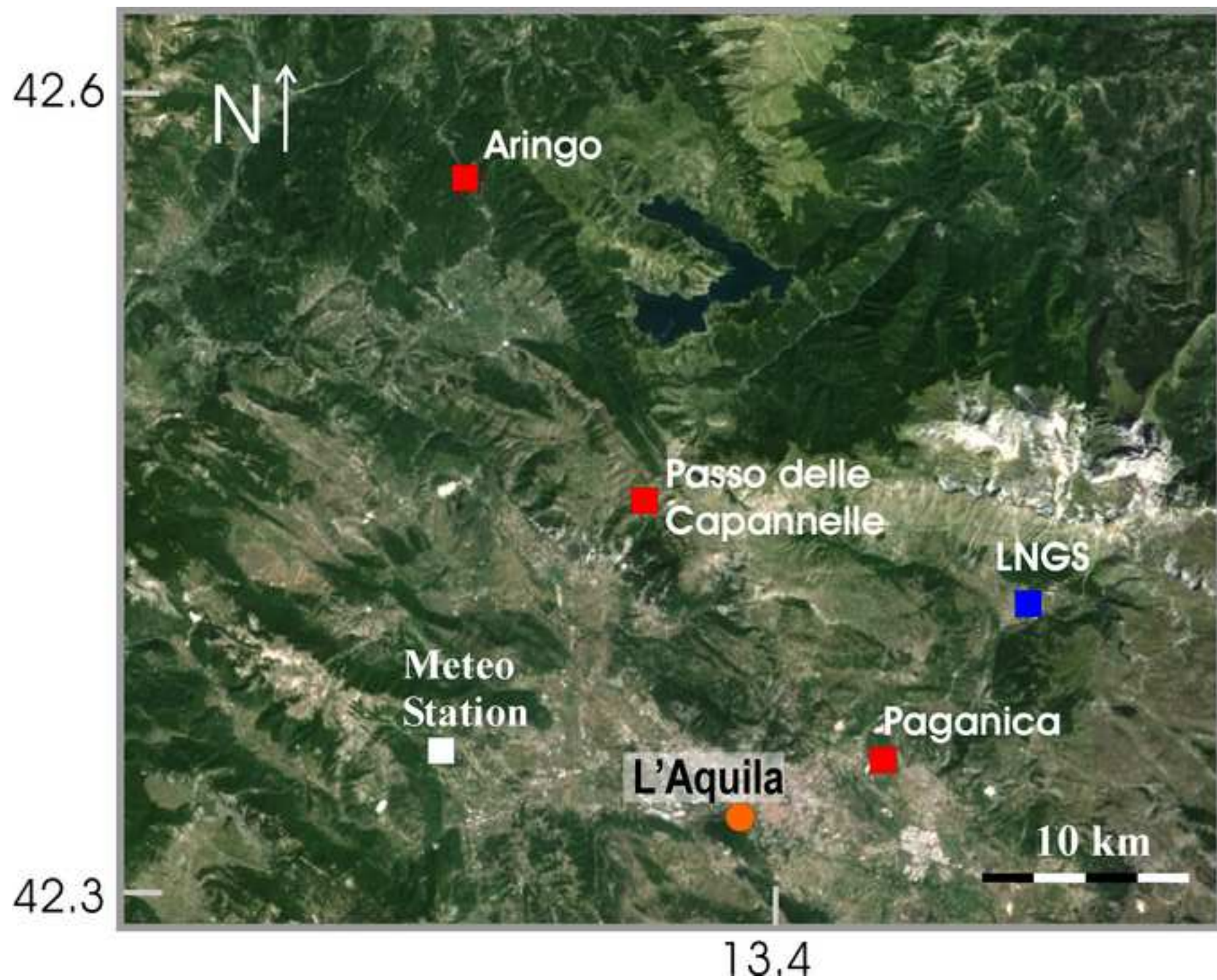
Figure 4
[Click here to download high resolution image](#)
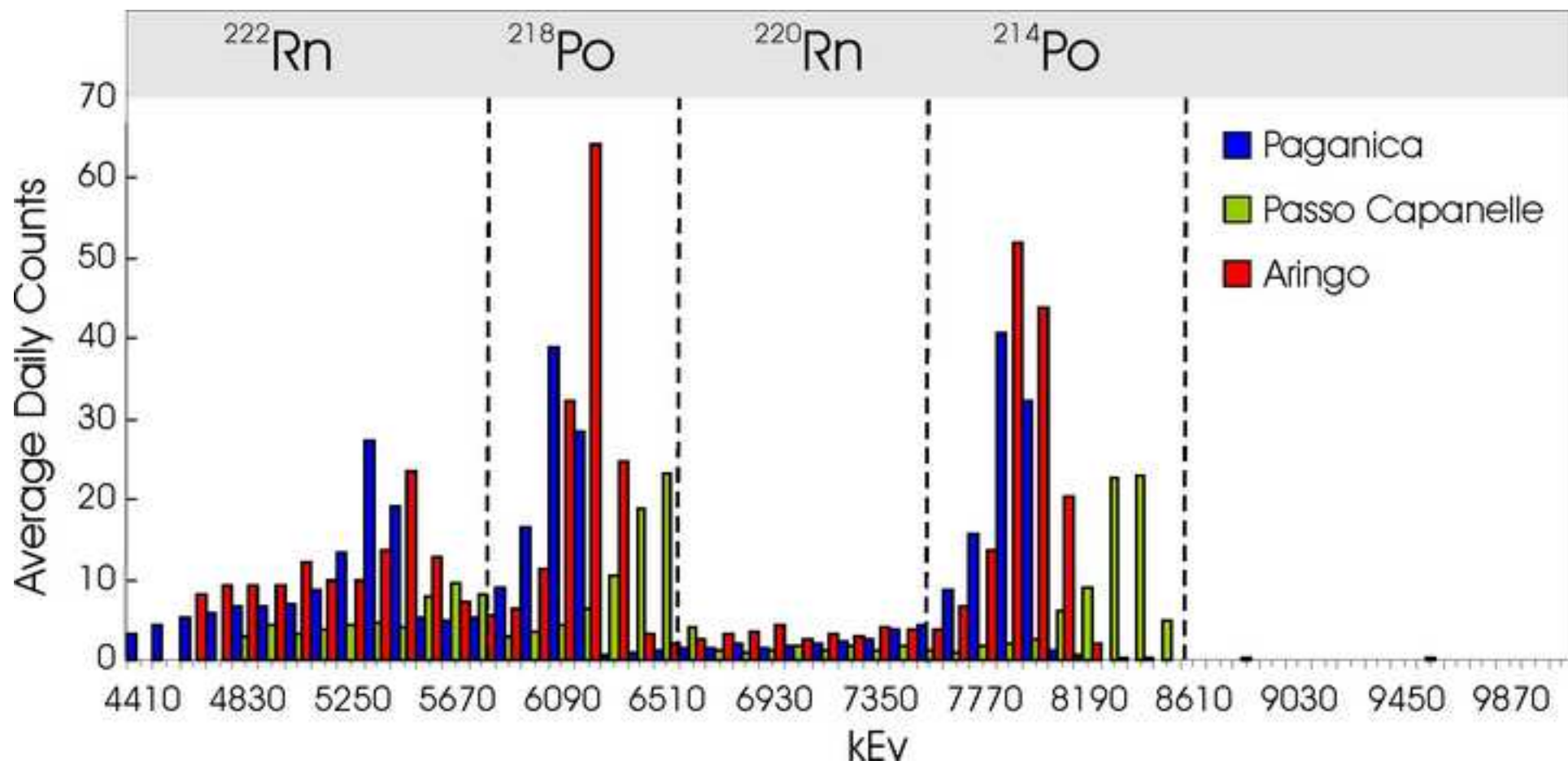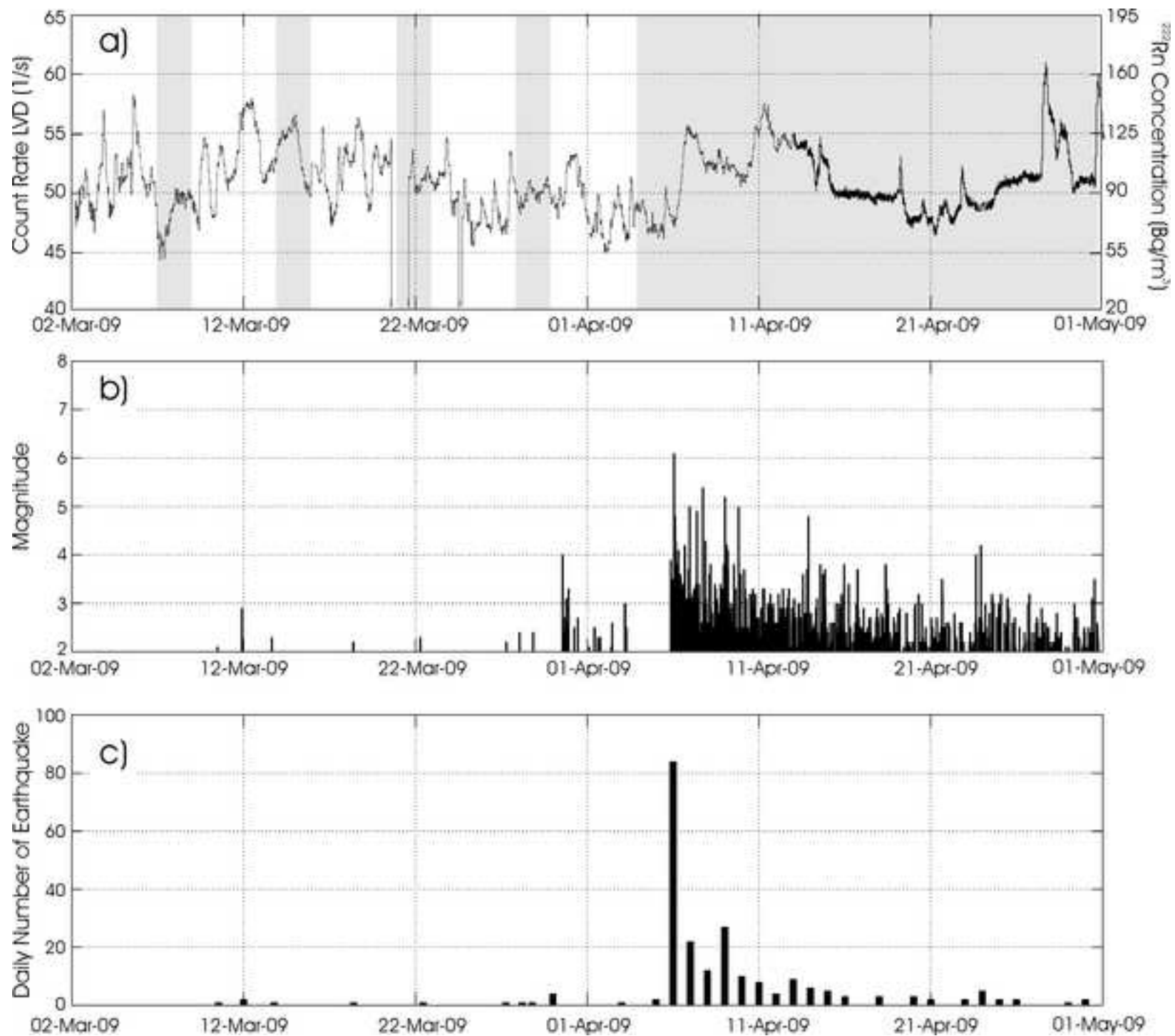
Figure 7
Click here to download high resolution image

Figure 7

Figure 8
Click here to download high resolution image

Figure 9
Click here to download high resolution image

Paganica - ^{222}Rn Concentration

^{222}Rn Measured ^{222}Rn Calculated ^{222}Rn Residuals
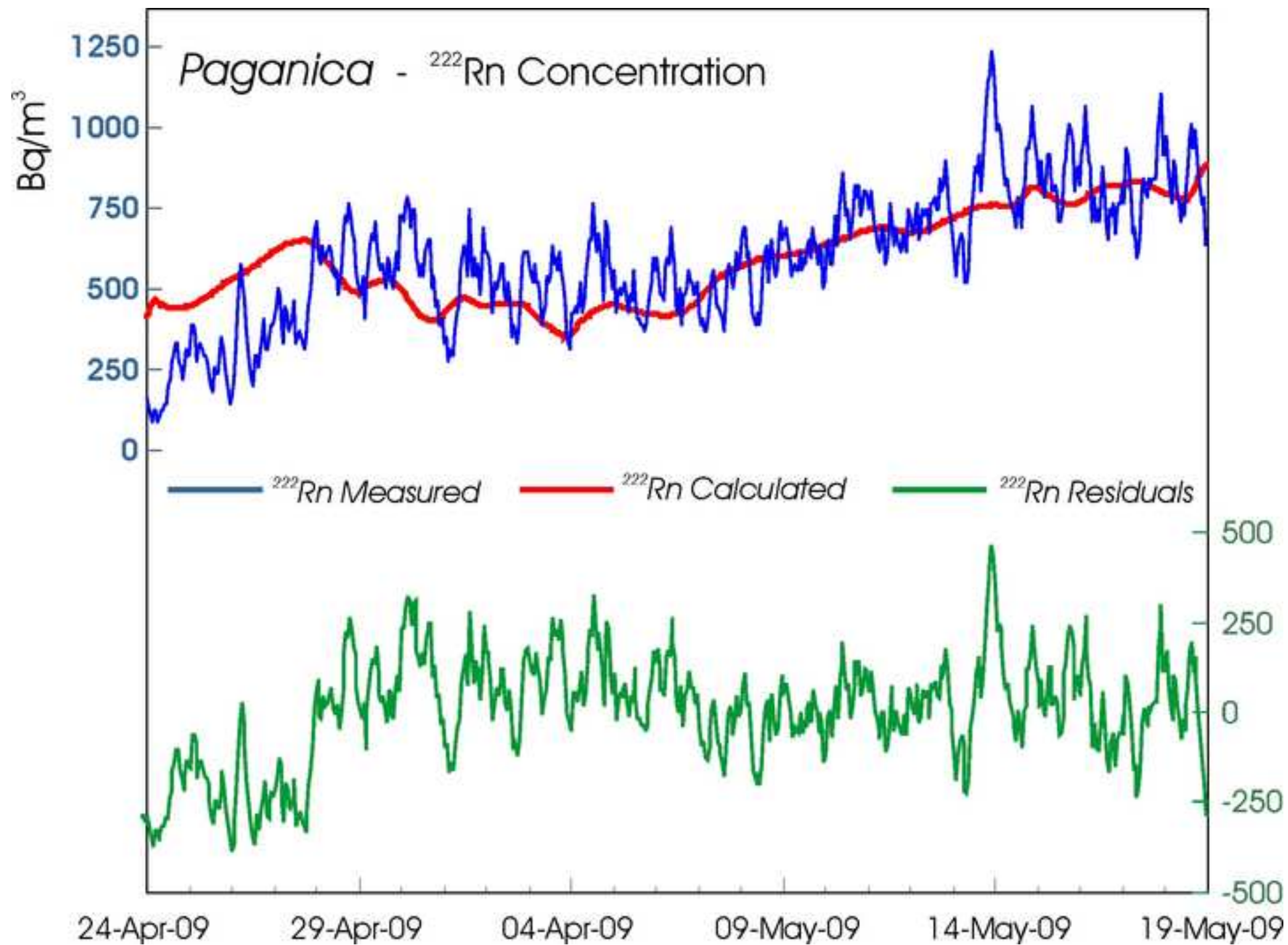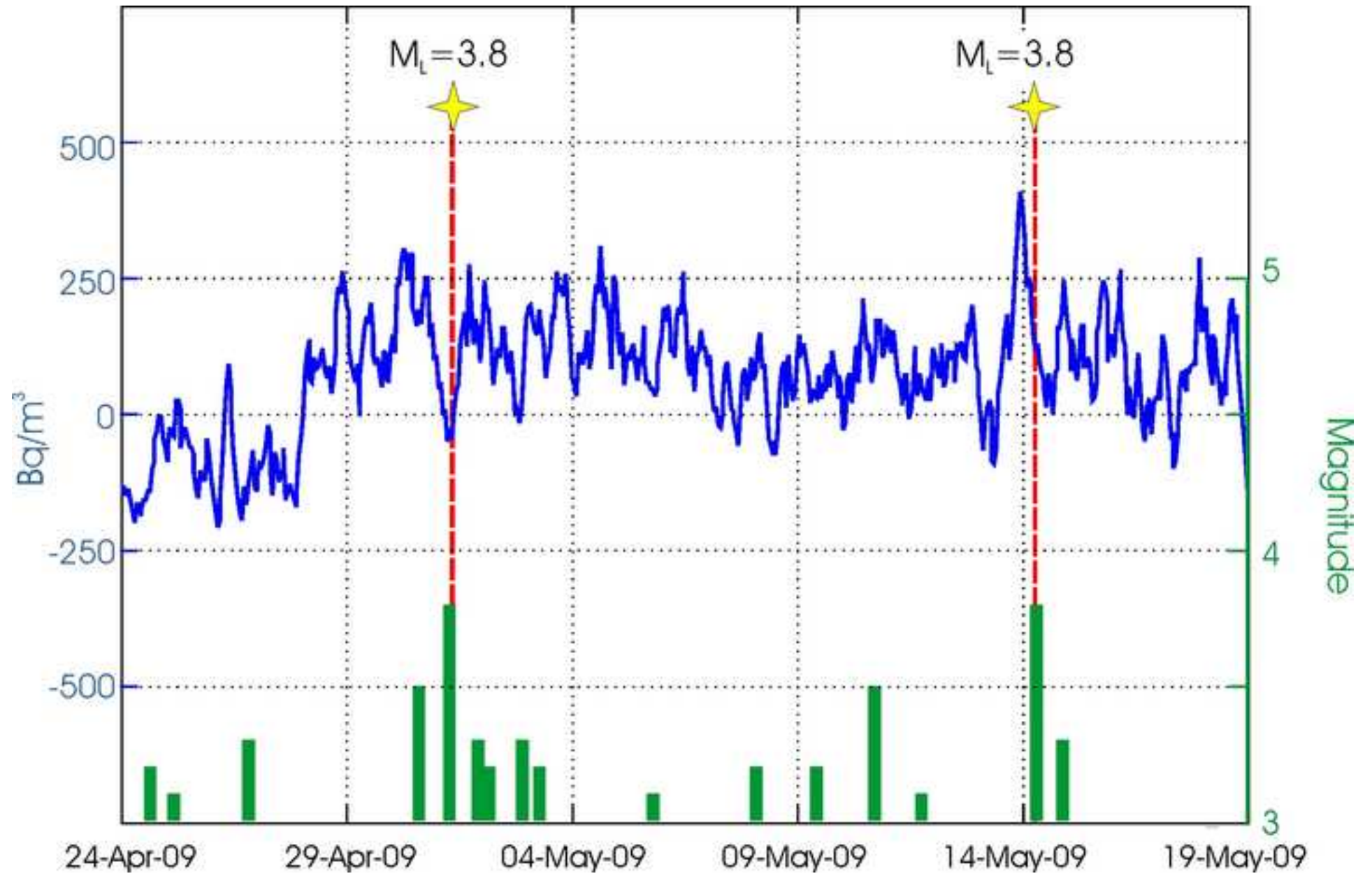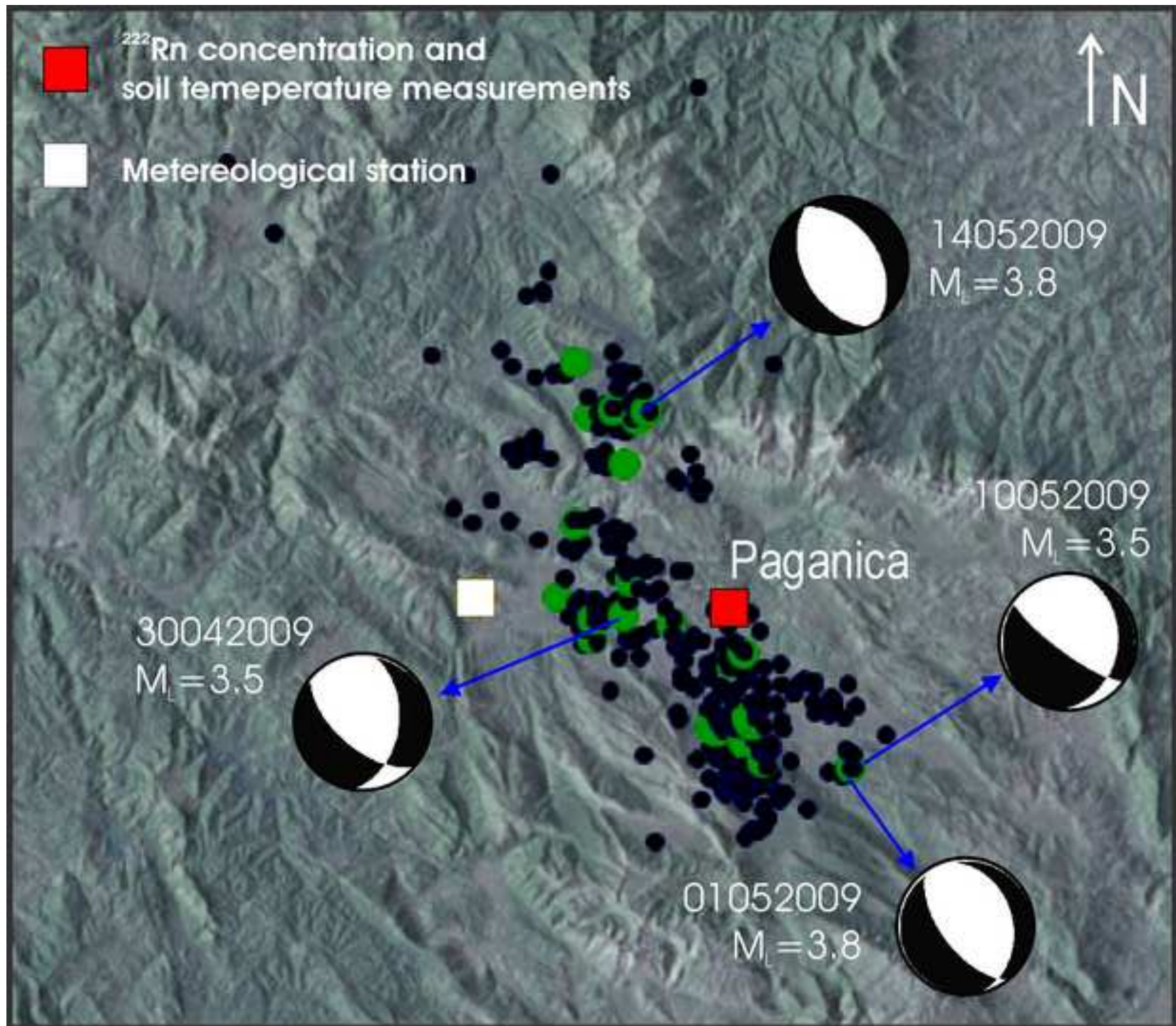
Figure 11
[Click here to download high resolution image](#)

Table 1. List of the ten higher earthquakes affected the Italian peninsula from the 1900 (INGV; www.ingv.it)

Time	Region	Magnitude (M_w)
28 December 1908	Messina Strict (Calabria, Sicily)	7.2
08 September 1905	Calabria	7.1
13 January 1915	Avezzano (Abruzzo)	7
23 November 1980	Irpinia (Campania, Basilicata)	6.9
23 July 1930	Irpinia (Campania)	6.7
07 September 1920	Garfagnana (Tuscany)	6.5
06 May 1976	Friuli	6.4
06 April 2009	Abruzzo	6.3
29 June 1919	Mugello (Tuscany)	6.2
21 August 1962	Irpinia (Campania)	6.2

Table 2. Daily correlation coefficients between ^{222}Rn concentration measured at Paganica station (see Figure 3) and the metereological parameters

		^{222}Rn Bq/m^3	Soil T °C	Air T °C	Air Prs mBar	Air H %	Wind Sp km/h
^{222}Rn	Bq/m^3	1.000	0.808	0.705	0.065	-0.263	-0.054
Soil T	°C	0.808	1.000	0.958	0.300	-0.200	-0.123
Air T	°C	0.705	0.958	1.000	0.384	-0.309	-0.044
Air Prs	mBar	0.065	0.300	0.384	1.000	-0.393	0.074
Air H	%	-0.263	-0.200	-0.309	-0.393	1.000	-0.724
Wind Sp	km/h	-0.054	-0.123	-0.044	0.074	-0.724	1.000